Journal of Illusion

PHENOMENAL REPORT

The static spin illusion

Saleeta Qadir* and Bernhard Egger

Cognitive Computer Vision Lab, Visual Computing Erlangen, Friedrich-Alexander-Universität Erlangen-Nürnberg

Abstract

We propose the static spin illusion, an extension of the motion without movement effect to the third dimension. Static two-dimensional images can be converted into three-dimensional spinning motion illusions using phase-shifted filters and AI-generated depth estimations. By modulating the motion amplitude based on depth, the approach creates perception of three-dimensional movement while maintaining static object positioning. The technique combines second derivative Gaussian filters with their Hilbert transforms, enhanced by depth-dependent speed modulation using depth estimation. The resulting video leads to a perceived 3D rotation for a static person. The proposed illusion won the illusion of the year contest 2024. We share the code to reproduce our illusion and create own variants. The posting can be found here: https://illusionoftheyear.com/cat/top-10-finalists/2024/.

Keywords: static spin illusion; illusory motion; motion without movement; depth perception; phase modulation

Edited by:
Arthur Shapiro, American University, USA

Reviewed by:
Yuki Kobayashi, Ritsumeikan University, Japan

Shin'ya Nishida, Kyoto University, Japan

Received: 15 November 2025; Revised: 6 May 2026; Accepted: 11 May 2026; Published: 27 November 2026

Freeman, Adelson, and Heeger introduced 'motion without movement' in 1991 as a term for a process to generate patterns that appear to move continuously without changing their positions (Freeman et al., 1991). Their procedure uses standard image processing steps, in particular, a quadrature pair of oriented filters to modulate local phase to create the illusion of motion by systematically introducing phase shifts into edge structures.

The underlying concept goes back to Shadlen and Carney, who demonstrated a cyclopean illusion where static flickering patterns presented to each eye resulted in the perception of movement (Shadlen & Carney, 1986). Their results concluded that the visual system combines image components differing by 90 degrees in spatial and temporal phase to compute motion direction.

The phenomenon of illusory motion in static images has been studied for several decades. Seminal works by Anstis (1970) and Anstis and Rogers (1975) established the foundational mechanics of the Reverse Phi effect, which has been further explored in various configurations, including the 'Perpetual Diamond' (Flynn & Shapiro, 2018) and configurational coincidence in geometric illusions (Kitaoka, 2006), visual dissociations between movement and stereo depth (Gregory & Heard, 1983), and second-order processing of four-stroke motion (Mather & Murdoch, 1999). The outcome is continuity of motion perception due to motion detectors in the human visual system resolving perceptual conflict between feature tracking and motion signals (Adelson & Bergen, 1985). An insightful overview of related motion illusions can be found under https://jake.vision/blog/motion-illusions.

The 'motion without movement' technique can be interpreted as a generalized variant of such illusions as it can be applied to images directly and not only lines that form simple geometric objects. The original 'motion without movement' technique creates motion effects but operates without consideration of depth information and is limited to 2D motion such as translation and rotation. For realistic three-dimensional motion perception, depth cues such as motion parallax become crucial, where objects at different depths exhibit differential motion patterns relative to an observer's position.

This work extends the classical motion without movement approach by incorporating depth information to create the percept of a three-dimensional motion,, like a 3D rotation. We modulate the motion amplitude based on computed depth maps, creating spatially varying effects that simulate realistic motion parallax, resulting in a perceived spinning motion.

*Correspondence: *Saleeta Qadir. Email: saleeta.qadir@fau.de

Journal of Illusion 2026. © 2026 Saleeta Qadir and Bernhard Egger. This is an Open Access article distributed under the terms of the Creative Commons CC-BY-NC-ND 4.0 license (https://creativecommons.org/licenses/by-nc-nd/4.0/), allowing third parties to copy and redistribute the material in any medium or format and to remix, transform, and build upon the material for any purpose, even commercially, provided the original work is properly cited and states its license.

In contrast to many optical illusions, the 'motion without movement' effect as well as our proposed illusion does not require to be manually adapted to a new image, but the proposed steps can be automatically applied to images of various centered objects to reach the same rotation effect for those.

This work has also been awarded first prize worldwide in the 'Illusion of the year' competition 2024 hosted yearly by the Neural Correlate Society.

Methodology

Our approach consists of four main stages: image preprocessing, depth map generation and enhancement, quadrature filter implementation, and phase modulation synthesis. Figure 1 illustrates the complete processing pipeline from the input image to the final motion illusion video. Our method builds on the motion without movement illusion but in addition steers the image manipulation by the depth to reach a perceived 3D motion. Although we can measure depth for a scene with 3D scanners, we use an AI-based estimation of depth instead. This enables to generate illusions from a huge variety of images and does not require expensive 3D capture.

Motion perception and visual illusions

The 2D illusion of 'motion without movement' (Freeman et al., 1991) creates the perception of global motion through local phase shifts. This uses oriented quadrature filters: the second derivative of a Gaussian filter (G_2) and its Hilbert transform (H_2), identical in structure except for a 90-degree phase shift. The sequence of phase-shifted filters follows:

$$F(t) = \cos(\omega t)G_2 + \sin(\omega t)H_2 \quad (1)$$

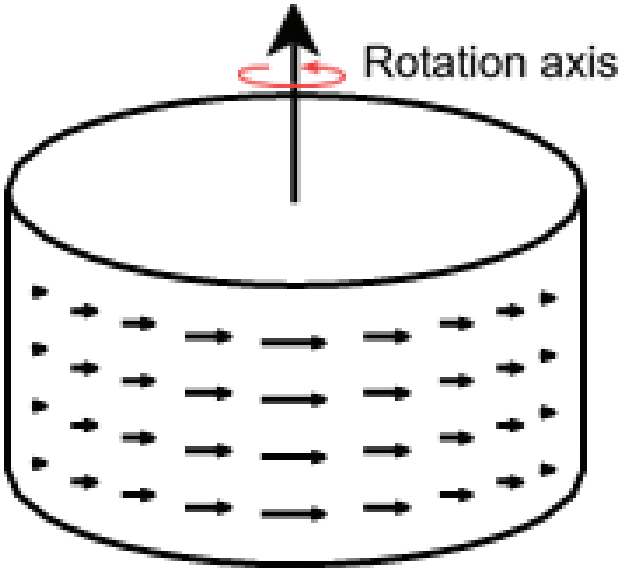


Fig. 1. Complete processing pipeline showing the transformation from static input image to three-dimensional motion illusion through depth estimation, filter processing, and phase modulation.

where F is the phase-shifted filter, ω is the rate of phase shift, and t is time.

Depth cues

Motion parallax is often discussed in terms of lateral translation, but it can also be applied to the perception of 3D rotation. When an object is rotated, points on the surface of the object that are physically closer to the observer and moving toward or away from the line of sight will exhibit a faster velocity compared to points further from the observer.

The perception of 3D rotation in this illusion is driven by the spatial variation of local motion signals. While often discussed in terms of motion parallax, the variation in perceived speed in a rotating cylinder Fig. 2 is primarily a result of the projection of tangential velocity onto the 2D image plane.

Points on the surface closest to the viewer move nearly perpendicular to the line of sight, resulting in a maximum 2D velocity projection. Conversely, as points approach the sides of the cylinder, their 3D motion becomes increasingly parallel to the observer's line of sight. Consequently, the projection onto the image plane decreases, causing the apparent slowing of motion at the lateral edges. This gradient of projected speeds, combined with depth-dependent direction, provides the primary cue for 3D rotation.

Image pre-processing

To prepare an image for this illusion, we first establish a desired motion direction, for example, from right to left. We also convert the image to grayscale, as some color combinations weakened the effect. The illusion works most effectively with high-contrast edges and differences in brightness, similar to how a bold line drawing can create a sense of movement.

We here focus the rotation effect around an axis in the center of the image. The rotation angle is provided as an input parameter to allow the user to define the overall direction of the scene relative to the desired spinning motion (we choose a vertical rotation axis). This enables the subsequent use of phase shifts to create a perceived spinning effect around the chosen axis in the final output. Images are converted to grayscale to bring out luminance-based edge features essential to effective phase shift use. While grayscale conversion is easier and emphasizes luminance information, the basic principles of this method apply to color images by applying the filters to individual color channels or a luminance channel derived from the color image.

To reach different rotation directions we can either rotate the input image or the filters. We choose to rotate the image and interpolate the pixels using nearest-neighbor interpolation for simplicity, rather than using steerable filters.

Citation: Journal of Illusion 2026, **6**: 13468 - https://doi.org/10.47691/joi.v6.13468

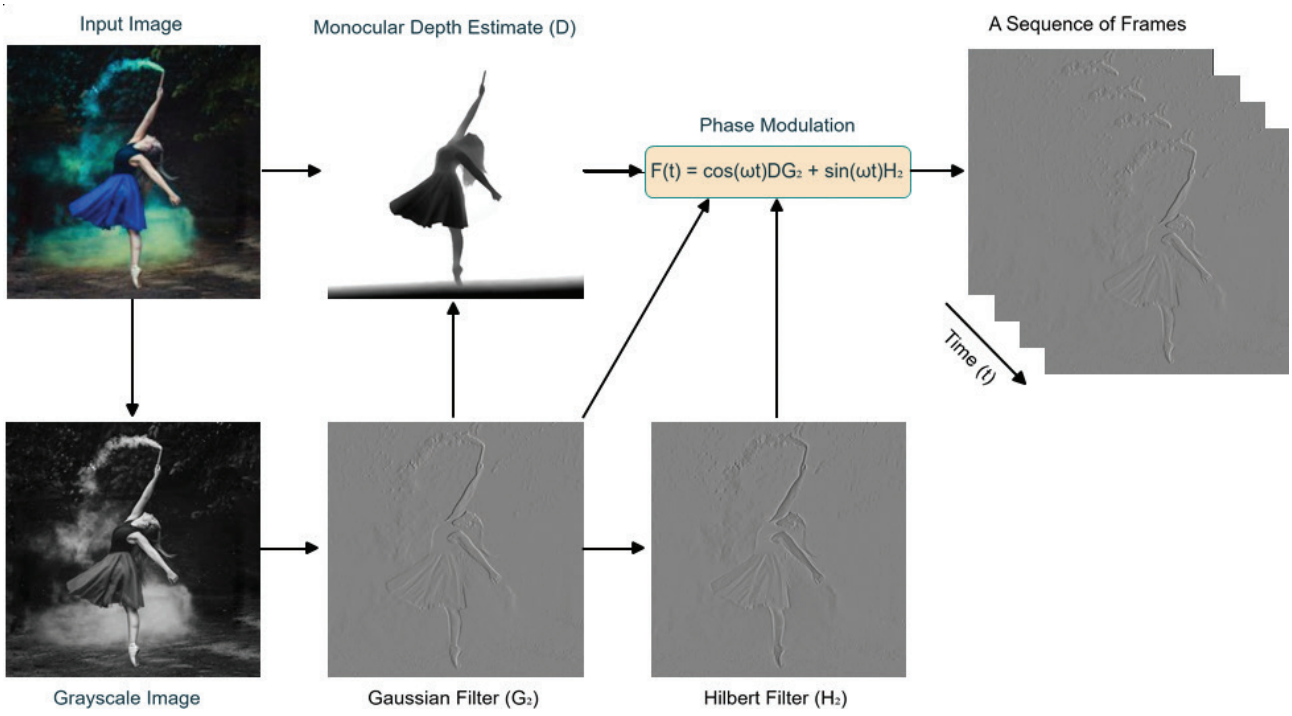


Fig. 2. Illustration of perceived tangential velocity on a rotating cylinder. The cylinder rotates around its central vertical axis (dashed line). Arrow lengths depict velocity relative to the viewer. Points on the surface closer to the viewer (e.g. at the front/center) exhibit longer arrows, signifying a higher speed. Conversely, points further from the viewer (e.g. at the sides) exhibit shorter arrows, indicating lower perceived speed.

The chosen interpolation method employed significantly impacts the quality of the final output. Nearest-neighbor interpolation, although computationally easier, preserves abrupt edges that are necessary to maintain the illusion. Other interpolation methods, such as bilinear or bicubic, create smoothing that diminish sharp details in transitions that are crucial for optimal phase shift perception.

Depth map generation

To make the illusion truly three-dimensional, we first need to understand how far away different parts of the image are. We use an AI model to estimate the depth of every object, creating a 'depth map' – a grayscale image where brightness corresponds to distance. However, the raw map from the AI might have a compressed range of values, making it hard to distinguish between objects at similar depths. To fix this, we remap or rescale these depth values. This process is like stretching out the grayscale tones to create more contrast, making the subtle differences in depth more distinct. This remapped depth map enhances the illusion, telling each part of the image how fast and in which direction to spin.

Depth information extraction utilizes Marigold, a zero-shot depth estimator based on diffusion models (Ke et al., 2024). Initial depth maps often exhibit insufficient variation in regions closer to the observer, appearing overly uniform. The post-processed depth maps demonstrate a more suitable distribution of values for representing near-field depth variations. Figure 3 illustrates the effect of this remapping, showing increased contrast and detail in regions closer to the observer.

We implement a selective adjustment of darker regions within the depth map (representing objects closer to the viewer) using triangle method thresholding to isolate them, followed by brightness adjustment and selective blending. Specifically, this involves converting the image to the LAB color space, extracting the lightness (L) channel, and then applying OpenCV's cv2.THRESH TRIANGLE method. This automated thresholding technique finds an optimal threshold by analyzing the image's histogram. It effectively segments the darker, typically closer, regions of the depth map, allowing for their targeted adjustment. The output of this remapping process is the normalized depth map D (eq. (2)). In this mapping, $D = 0$ corresponds to points located on the plane of the rotation axis. Values $D \in (-1, 0)$ represent points closer to the viewer than this plane, while $D \in (0, 1)$ represent points further away, enabling the differentiation of motion direction and speed.

Quadrature filter implementation

We use a pair of filters to create the sensation of movement in a static image. The first, a Gaussian filter



Fig. 3. On the left you see the depth map generated by Marigold. On the right you see the enhanced depth map, which is the result of the selective brightening process described in the text, and serves as the depth-modulation parameter (D) in eq. (2).



Fig. 4. On the left you see the G2 image generated. On the right you see the consequent H2 image generated from the G2 image.

combined with a second derivative operation, acts like a lens that specifically highlights the sharpest edges by isolating high-frequency spatial gradients. The second, its Hilbert transform, provides an identical map of those same edges but with a subtle shift. By rapidly alternating between these two slightly different views of the edges, we trick the brain into perceiving motion that isn't really there. However, this process can cause an unwanted effect known as aliasing. To prevent this, we use an additional step (Sobel filtering) to isolate the primary edge gradients. While Sobel is a high-pass operation, it effectively prunes low-amplitude noise and background gradients that can cause visual smearing during the digital Hilbert transformation. To mitigate these artifacts, we applied Sobel filtering before the Hilbert transformation to emphasize the primary directional energy of the G_2 filtered image.

The method employs oriented quadrature filters consisting of a second derivative Gaussian filter G_2 and its Hilbert transform H_2. The Gaussian standard deviation $\sigma = 0.1$ was established as optimal for the standardized maximum resolution inputs. A second derivative Gaussian filter is applied to the grayscale input image to isolate edges. Figure 4 illustrates the Gaussian-filtered image on the left and the corresponding Hilbert-transformed image on the right. Visual artifacts are evident in the latter, resulting from the frequency response limitations of the digital Hilbert transform implementation, which can cause smearing when processing broad, low-frequency gradients. To mitigate these artifacts, we applied Sobel filtering before the Hilbert transformation to emphasize the primary directional energy and isolate the sharp edge structures that the digital transform can process without distortion. As shown in Fig. 5, this results in an alias-free 90 degree phase shifted image.

Citation: Journal of Illusion 2026, **6**: 13468 - https://doi.org/10.47691/joi.v6.13468



Fig. 5. Left: Input image processed with a Sobel filter and followed by the second derivative of a Gaussian. Right: Hilbert transform applied to the processed image on the left.

Phase modulation and motion synthesis

Phase modulation creates the perceived spinning motion illusion through temporal variation:

$$F(t) = \cos(\theta t) \cdot D \cdot G_2 + \sin(\theta t) \cdot H_2 \quad (2)$$

where G_2 represents the Gaussian-filtered image, H_2 denotes the Hilbert-transformed component, and θ controls the base rate of phase shift, directly governing the overall speed of the perceived motion. The crucial innovation lies with D, which corresponds to the enhanced depth map. The depth map D is normalized between −1 and 1, where the furthest objects receive values of −1 (causing motion in one direction) and the closest objects receive values of 1 (causing motion in the opposite direction). This depth-dependent modulation of D on the Gaussian component (G_2) dynamically alters both the perceived speed and direction of the spinning motion for each pixel, based solely on its depth value. As a theoretical alternative to eq. (2), speed could be modulated directly via the phase rate: $F(t) = \cos(\theta t \cdot D)G_2 + \sin(\theta t \cdot D)H_2$. While this formulation may offer a more direct mapping to perceived 3D velocity, the current work utilizes amplitude modulation, and a comparative study of these two approaches is left for future investigation. The rotation is fixed around a vertical axis located within the image plane that passes through its exact center. This central axis is the point of zero rotation, with rotational motion increasing in magnitude as pixels move further away from this central point. This creates the three-dimensional effect.

Conclusion

This work demonstrates creating three-dimensional motion illusions from static images using phase-shifted filters and AI-generated depth maps. The key innovation lies in depth-dependent phase modulation that creates spatially varying motion amplitudes corresponding to scene depth structure. The resulting illusion leads to a strong effect of a perceived 3D motion and further emphasizes the effectiveness of the 'motion without movement' technique.

Data availability

The source code for this work is publicly available at https://github.com/saleeta/The-Static-Spin. The implementation includes depth map generation, filter processing, and motion synthesis components necessary for reproducing the results presented in this work or creating your own illusion based on a different image. A demonstration video illustrating the static spin illusion can be viewed at http://www.youtube.com/watch?v=SPNykV3BV8E.

Conflict of interest and funding

The authors declare no conflicts of interest. This research received no external funding.

References

Adelson, E.H. & Bergen, J.R. (1985). Spatiotemporal energy models for the perception of motion. *Journal of the Optical Society of America, 2*(2), 284–299. https://doi.org/10.1364/JOSAA.2.000284

Anstis, S.M. (1970). Phi movement as a subtraction process. *Vision Research, 10*(12), 1411–1430. https://doi.org/10.1016/0042-6989(70)90092-1

Anstis, S.M. & Rogers, B.J. (1975). Illusory reversal of visual depth and movement during changes of contrast. *Vision Research, 15*, 957–961. https://doi.org/10.1016/0042-6989(75)90236-9

Flynn, O. & Shapiro, A. (2018). The perpetual diamond: Contrast reversals along thin edges create the appearance of motion in objects. *i-Perception*, *9*, 204166951881570. https://doi.org/10.1177/2041669518815708

Freeman, W., Adelson, E., & Heeger, D. (1991). Motion without movement. *ACM SIGGRAPH Computer Graphics, 25*(4), 27–30, https://doi.org/10.1145/127719.122721

Gregory, R.L., & Heard, P.F. (1983). Visual dissociations of movement, position, and stereo depth: some phenomenal phenomena. *Quarterly Journal of Experimental Psychology, 35*(Pt 1), 217–237. https://doi.org/10.1080/14640748308402127

Ke, B., Obukhov, A., Huang, S., Metzger, N., Daudt, R.C., & Schindler, K. (2024). Repurposing diffusion-based image generators for monocular depth estimation. In *2024 IEEE/CVF Conference on Computer Vision and Pattern Recognition (CVPR), 17–21 June 2024* (pp. 9492–9502). IEEE, Piscataway, NJ, USA.

Kitaoka, A. (2006). Configurational coincidence among six phenomena: a comment on van Lier and Csath´o (2006). *Perception, 35*(6), 799–806. https://doi.org/10.1068/p5319b

Mather, G., & Murdoch, L. (1999). Second-order processing of four-stroke apparent motion. *Vision Research, 39*(10), 1795–1802. https://doi.org/10.1016/S0042-6989(98)00191-6

Shadlen, M. & Carney, T. (1986). Mechanisms of human motion perception revealed by a new cyclopean illusion. *Science, 232*(4746), 95–97. https://doi.org/10.1126/science.3952502